2014-07

A novel real-time non-linear wavelet-based model predictive controller for a coupled tank system

Owa, K

10.1177/0959651813520149

Proceedings of the Institution of Mechanical Engineers, Part I: Journal of Systems and Control Engineering

SAGE Publications

Original Article

PROCEEDINGS OF THE INSTITUTION OF MECHANICAL ENGINEERS
PART I: JOURNAL OF SYSTEMS AND CONTROL ENGINEERING

Proc IMechE Part I:
J Systems and Control Engineering
2014, Vol. 228(6) 419–432

DOI: 10.1177/0959651813520149
pii.sagepub.com
SAGE

A novel real-time non-linear wavelet-based model predictive controller for a coupled tank system

Kayode Owa[1,2], Sanjay Sharma[1,2] and Robert Sutton[1,2]

Abstract

This article presents the design, simulation and real-time implementation of a constrained non-linear model predictive controller for a coupled tank system. A novel wavelet-based function neural network model and a genetic algorithm online non-linear real-time optimisation approach were used in the non-linear model predictive controller strategy. A coupled tank system, which resembles operations in many chemical processes, is complex and has inherent non-linearity, and hence, controlling such system is a challenging task. Particularly important is low-level control where often instability and oscillatory responses are observed. This article designs a wavelet neural network with high predicting precision and time–frequency localisation characteristics for an online prediction model in the non-linear model predictive controller to show the effectiveness of this approach in controlling the liquid at low level. To speed up the training process, a fast global search stochastic non-linear conjugate wavelet gradient algorithm is initially used to train the wavelet neural network structure before the genetic algorithm optimisation technique is utilised to tune adaptively the wavelet neural network parameters. The non-linear model predictive controller algorithm is tested for both approaches: first, in a simulation using identified models, and second, in a real-time practical application to a single-input single-output system coupled tank system. The results show an excellent control performance with respect to mean square error and average control energy values obtained.

Keywords

Wavelet neural network, artificial neural network, modelling, system identification, non-linear model predictive control, real-time practical implementation, genetic algorithms, single input single output, non-linear optimisation, coupled tank system, Simulink model

Date received: 23 September 2013; accepted: 11 December 2013

Introduction

The control of fluids is one of the numerous challenging tasks in process industries.[1,2] Fluid level control is probably the most common control problem in practical process systems.[3] Many applications of fluid control can be found in chemical blending, level and flow control problems, temperature control in storage tanks, hot-water inputs, temperature stabilisations and reaction vessels.[4–6] A significant and challenging control problem is the infinitesimal precision control at low level of small amounts of fluid, which invariably tend to have a higher degree of non-linearity. This problem is further more complicated when operated under tight performance specifications to satisfy a number of constraints at the same time. This includes the control of printing quality for drop-on-demand ink-jet printers, which describe a technology that has been applied to printed circuit boards, organic transistors, DNA microarrays, and flat panel, plasma and light-emitting diode displays.[2] Another important use of small level of fluid control can be found moving coaxing fluids into desired spatial positions or acting as a medium for moving the positions of solid objects into desired spatial position or orientation[2] which also involves tiny amounts of fluid to be controlled. Other examples can be found in

[1]School of Marine Science and Engineering, Plymouth University, Plymouth, UK
[2]Marine and Industrial Dynamic Analysis Research (MIDAS) Group, Plymouth, UK

Corresponding author:
Kayode Owa, School of Marine Science and Engineering, Plymouth University, 3a Reynolds Building, Drake Circus, Plymouth PL4 8AA, UK.
Email: kayode.owa@plymouth.ac.uk; olayemi_owa@yahoo.co.uk

medical or biological systems which involve cerebrospinal fluid control systems,[7] low-level control of small flow intensity hydraulic fluid used to determine the pressure drop in the throttling aperture of a piezoelectric stack[8] and monitoring the parameters of Taylor flow in small channels using optical technique.[9]

In all these examples, it is important to note that an infinitely small amount of fluid needs to be controlled in order to achieve a particular aim and objective in their various applications. A coupled tank system (CTS) apparatus is used here to investigate the basic and advanced control engineering principles which include the study of static and dynamic systems[10] and the low-level control of fluids. The CTS is highly non-linear due to the feature characteristics of the valves, the fundamental dynamic equations which are time variant and the non-linear flow characteristics in the tank system.[3,11,12] Many researchers have investigated the CTS for control applications.[1,3,5] However, the aforementioned researches have not explored or demonstrated the use of the CTS to control a small amount of liquid, which will be achieved by maintaining a small level of liquid in the second tank. Complex non-linear behaviours exist at extremely low level of operations,[13] making the prediction performances of a process model more difficult.[14]

Over many years, classical control strategies such as the proportional–integral–derivative (PID) controller have been implemented, well established and stable.[6,15,23] However, PID controllers are not always able to provide good and acceptable results, especially when the system exhibits non-linearities.[16,23] Moreover, a PID controller will have more difficulties in maintaining small level fluid control because of its tendency to overshoot.[17]

Most efficient process operations today require operating systems closer to the boundary of the admissible operating region,[18] and therefore, linear models are mostly insufficient to represent adequately the non-linear dynamics of the plant.[19,22] However, there have been further advancements in technology, and researchers have always been looking for new methods and approaches for greater and increased control efficiency.[13] To tackle the challenge of controlling a very small amount of fluid, an efficient and advanced control strategy is therefore needed to overcome these challenges for higher efficiency and production. Model predictive control (MPC) is an advanced control strategy that has the capabilities to handle all these mentioned challenges.[13] MPC has had a significant impact on its application because of its ability to control and optimise complex processes with constraints.[20] Model predictive controllers rely mainly on dynamic models of the process and therefore can use either a linear or a non-linear model representation of the plant for prediction purposes.

Many control strategies are often accomplished using linear techniques because linear models for controlling plants have been very well established[21] and invariably used in MPC strategies[6,10] over the past four decades.[18] A non-linear model gives a more accurate prediction in a wider operating range of control.[13] Artificial neural network (ANN) has been progressively used in many applications over the years.[24–26] Recently, the wavelet function is combined with an ANN and shown to learn faster than a conventional ANN.[27]

The wavelet function has become very powerful for signal analysis. It is similar to a Fourier transform, but the wavelet is more useful because it can easily provide not just the frequency but also the time space information of a complex function, which is very useful for many practical applications.[28] This time–frequency signal localisation is one major advantage as it helps in the ultimate search for a global minimum solution during the training process. A wavelet also has the capabilities of approximating functions that are difficult to approximate by other methods.[28] The wavelet neural network (WNN) is a kind of ANN constructed by a suite of wavelet bases replacing sigmoid functions. It realises the characteristic extraction of the signal through assigning weights to the inner product of wavelet base and signal vector.[29] Researchers have increasingly seized the opportunity to employ wavelet functions with its choice of different mother wavelets in various modelling disciplines and tasks.[29–31] Some of the widely used mother wavelets such as Morlet, Haar, Shannon, Mexican hat and Daubechies are chosen based on their diverse features. The work of Jahangiri et al.[31] was based on Mexican hat mother wavelet and was able to establish that neurons activated by wavelet functions in the ANN model are more effective than the sigmoid functions when modelling the single-input single-output (SISO) CTS.

The Morlet wavelet has been widely used in many applications such as climatic peak load forecasting,[29] short-term weather load forecasting[32] and stock market prediction[30] for better performances and faster convergence rate of WNN than traditional radial basis function.[32] There is no application of Morlet wavelets in CTS control in the literature. The excellent multi-resolution property of the Morlet wavelet used in other applications can be useful in this work where a WNN model will be used to extract the best features of CTS while operating at a very small low level. This information will be advantageous in non-linear model predictive control (NMPC) strategy for step ahead online plant prediction. This article shows that an excellent low-level control is achieved using WNN compared to other existing methods,[13,33] and results are verified both in simulation and in real-time implementation of NMPC strategy.

This article is organised as follows: section 'System identification' describes the system identification process, while section 'WNN modelling' gives the details of the WNN modelling procedures. Section 'Non-linear control strategy for CTS' reports on the non-linear control strategies employed. Section 'Results and discussion' discusses both simulation and real-time results. Finally, a concluding remark is provided in section 'Concluding remarks'.

System identification

It is not every time that the mathematical model equations for most control strategies are readily available. In addition, some complex mathematical model equations might be difficult to derive or there might be model mismatch. The use of mathematical model equations often results in an ineffective controller design because of the discrepancy error in the model equations and the real plant. Process plant degradation, manufacturer design errors, equipment wear and equipment tear are also part of the reasons for model equation mismatches with the real plant dynamics. In situations like this, system identification is usually a good technique to derive a black box model of the real plant and is in turn used to predict the behaviour of the plant.

The pump supplies fluid into the left tank (Tank 1) with valve A fully opened, while valve C (Tank 2) is opened in midway position and valve B in Tank 1 is in fully closed position. The voltage input, u_1, to the pump is the manipulated variable, while the voltage corresponding to the height or level of the fluid in Tank 2 is the controlled variable. This configuration defines the second-order SISO set-up used in this article. Here, raw measured input–output data are collected in open-loop practical experiment. Three sets of different input–output data of 2980 samples each were obtained from the SISO CTS with a sampling time of Ts of 0.2 s. These samples of data were collected and were taken in such a way to show both the fluid filling up and draining process in order to obtain the crucial plant details.

Combinations of pseudo-random binary sequence (PRBS) and uniformly distributed noise signals are used to excite the real plant at three different times, and the output responses obtained are shown in Figure 1. The first data set is for training (Figure 1(a)), the second data sample (Figure 1(b)) is for validation and the third data set (Figure 1(c)) is for testing the derived model.

Table 1 shows the means and the variances of the different sets of input signals used to excite the real plant.

These collected data will be used to derive non-linear black box models using both ANN and WNN approaches. The proposed WNN model will be discussed in the next section.

WNN modelling

The WNN has wavelet functions in the hidden layer, which is also referred to as a wavelet layer. Training of a WNN involves finding the unknown weights between input to hidden layer (WI_{ji}), hidden to output layer (WO_{kj}), translation factor (b_j) and dilation (expansion) factor (a_j).

In this work, a Morlet wavelet $\varphi(x)$ is selected as a mother wavelet. The wavelet $\varphi(x)$ is expressed in equation (1) and is used as the activation function for the neurons in the hidden layers of the WNN

$$\varphi(x) = \cos(1.75x)\exp\left(-\frac{x^2}{2}\right) \tag{1}$$

where x is expressed in equation (2) as

$$x = \frac{\sum_{j=1}^{L} WI_{ji}X_i^n - b_j}{a_j} \tag{2}$$

A wavelet transform allows exceptional localisation in the time domain via translation (a shifting process)

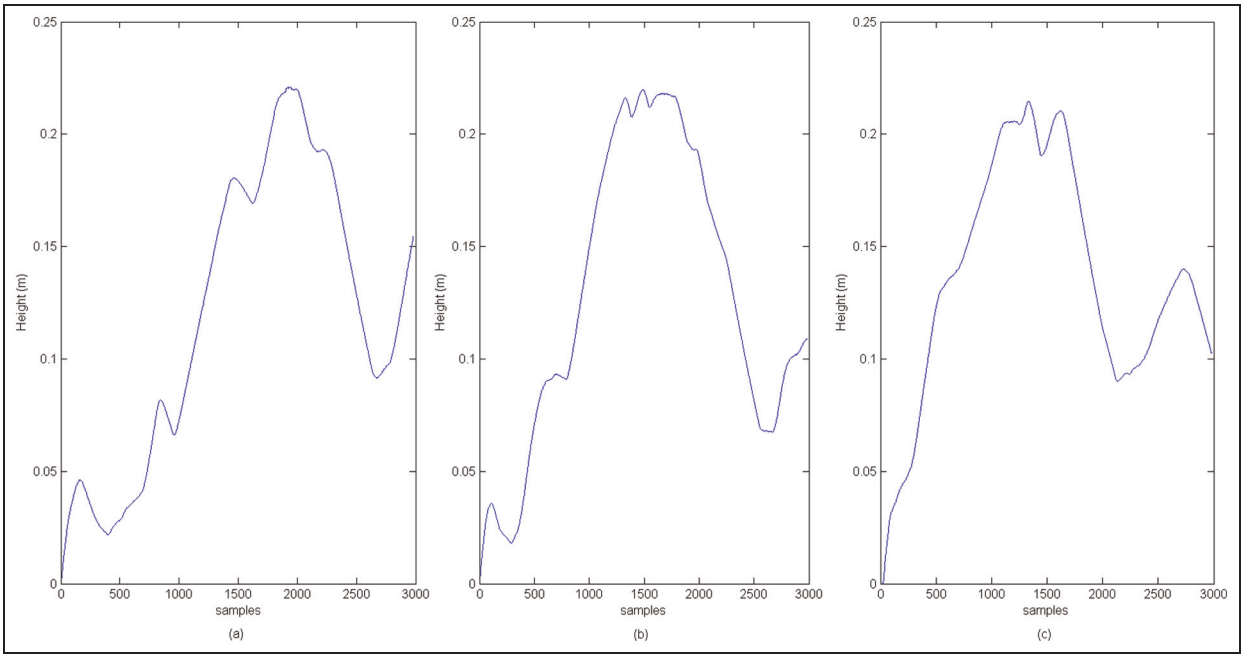

Figure 1. Output responses collected for training. (a) Plant open loop response data used for network Training; (b) Plant open loop response data used for network Validation; (c) Plant open loop response data used for network testing .

Table 1. Mean and variance values of the input signals.

Input data properties	First data (training)	Second data (validation)	Third data (testing)
Mean (V)	5.1935	4.9423	5.0259
Variance (V)	10.9190	10.7215	10.3617

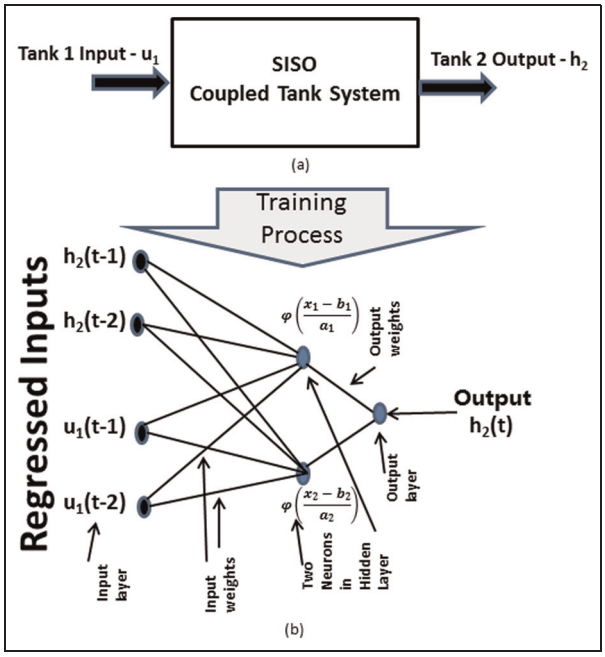

Figure 2. (a) Structure of SISO CTS and (b) SISO WNN training structure.
SISO: single-input single-output; WNN: wavelet neural network.

and also in the frequency domain via dilation (a scaling process) of the mother wavelet. The effect of these shifting and scaling processes is to produce a time–frequency representation of the signal. The wavelet basis functions are shifted in time domain to maintain the same number of oscillations, and its frequency is scaled in amplitude to maintain energy. Owing to their capability to localise in time, wavelet transforms readily lend themselves to non-stationary signal analysis. The SISO CTS block diagram is shown in Figure 2(a), while the architecture structure of SISO WNN used for the training in order to derive the non-linear model is shown in Figure 2(b). Here, the inclusion of wavelet activation functions in the hidden layer unlike the traditional ANN with biases weights in the layer structures. An initial heuristic study was conducted to ascertain the optimal number of parameters of the WNN, which is represented in a non-linear autoregressive with eXogeneous inputs (NARX) form of $y_{model} = f(h_2(t-1), h_2(t-2), u_1(t), u_1(t-1))$, where $f(\cdot)$ is an unknown complex non-linear function. Here, 2-neuron, 2-input and 2-output delays give a total of 14 unknown parameters in the WNN structure. The training data set consists of two sequences of vector, which is the total number of samples of input–output data set which are the input sequence u_1 and the measured process output h_2 which are re-arranged in a regressed form (Figure 2(b)) of the specified number of 2-input and 2-output delay. This gives a constant feedback memory of previous input–output value process during the training process.

The aim here is to create a WNN model by finding the optimised unknown parameters as expressed in equation (3), where the WNN model output is y_{model}

$$y_{model} = \sum_{j=1}^{N} \prod_{i=1}^{P} w_i \varphi_i + \sum_{i=1}^{S} \prod_{o=1}^{Q} net_i w_o \tag{3}$$

The term $(\delta\varphi(x)/\delta x)$ in equation (4) is the derivative of equation (1). This will be used as part of the terms for calculating the partial derivatives of the error $\in$ functions in equation (5)

$$\frac{\delta\varphi(x)}{\delta x} = -[x*\cos(1.75*x) + 1.75\sin(1.75*x)]*\exp\left(-\frac{x^2}{2}\right) \tag{4}$$

The partial derivatives of the unknown weights WI_{ji}, WO_{kj}, b_j and a_j are calculated in equation (9) by using conjugate stochastic gradient method

$$\frac{\delta \in}{\delta WI_{ji}} = \sum_{n=1}^{N}\sum_{k=1}^{S}\left[\left(y_{model_k}^n - y_{target_k}^n\right)*WO_{kj}*\frac{\partial\varphi(x)}{\partial x}\frac{X_i^n}{a_j}\right]$$

$$\frac{\delta \in}{\delta WO_{kj}} = \sum_{n=1}^{N}\left(y_{model_k}^n - y_{target_k}^n\right)*\varphi\left[\frac{\sum_{i=1}^{L} WI_{ji}X_i^n - b_j}{a_j}\right]$$

$$\frac{\delta \in}{\delta a_j} = \sum_{n=1}^{N}\sum_{k=1}^{S}\left(y_{model_k}^n - y_{target_k}^n\right)*WO_{kj}*\frac{\partial\varphi(x)}{\partial x}\left[\frac{\sum_{i=1}^{L} WI_{ji}X_i^n - b_j}{a_j^2}\right]$$

$$\frac{\delta \in}{\delta a_j} = \sum_{n=1}^{N}\sum_{k=1}^{S}\left(y_{model_k}^n - y_{target_k}^n\right)*WO_{kj}*\frac{\partial\varphi(x)}{\partial x}\left[\frac{\sum_{i=1}^{L} WI_{ji}X_i^n - b_j}{a_j^2}\right] \tag{5}$$

where N is the number of samples to be trained, S is the number of outputs and L is the number of regressed inputs in the WNN structure.

The partial derivatives are subsequently used to update the unknown weights using the formulas in equation (6)

$$
\begin{aligned}
WI_{ji}^{ii+1} &= WI_{ji}^{ii} - \gamma_a \frac{\partial \in}{\partial WI_{ji}^{ii}} \\
WO_{kj}^{ii+1} &= WO_{kj}^{ii} - \gamma_a \frac{\partial \in}{\partial WO_{kj}^{ii}} \\
b_j^{ii+1} &= b_j^{ii} - \gamma_b \frac{\partial \in}{\partial b_j^{ii}} \\
a_j^{ii+1} &= a_j^{ii} - \gamma_b \frac{\partial \in}{\partial a_j^{ii}}
\end{aligned} \tag{6}
$$

The training of the feed forward WNN is based on the minimisation of the error between the model and the target as shown in equation (7)

$$
MSE = \sum_{n=1}^{N} \sum_{k=1}^{S} \frac{\left(y_{model_k^n} - y_{target_k^n}\right)^2}{2*N} = \sum_{n=1}^{N} \frac{e^{n2}}{2*N} \tag{7}
$$

As the training progresses, validation process is constantly carried out. The WNN is initially trained using conjugate stochastic gradient method, and the training stops when the validation model error value starts increasing. The optimal weight derived from this stage is used to generate an initial 100 population for a genetic algorithm (GA) which was run for 500 generations to obtain the optimal values of the unknown parameters of the WNN. The ANN model is also obtained in similar manner, and it is used for benchmarking purpose in this article.

Non-linear control strategy for CTS

MPC is a form of an advanced control strategy where a finite prediction horizon open-loop optimal control problem is derived by obtaining a real-time solution online at each sampling instant. The optimisation yields an optimal control sequence, and the first value in this sequence is applied to the real plant.

The MPC strategy was implemented here by using a GA as the optimisation approach and the non-linear WNN model as a predictor. The schematic picture of the process is shown in Figure 3.

The predictor's task is to predict the plant outputs based on the regressed inputs at every instant. This is done for different control moves within a prediction range. The value of the control horizon should always be less than the prediction horizon. The GA is used to solve and minimise the complex real-time optimisation (RTO) cost function (see equation (8)) at every sampling time to determine the optimum control inputs that give the least error between the predicted output and the trajectory reference signals and minimise the controller efforts

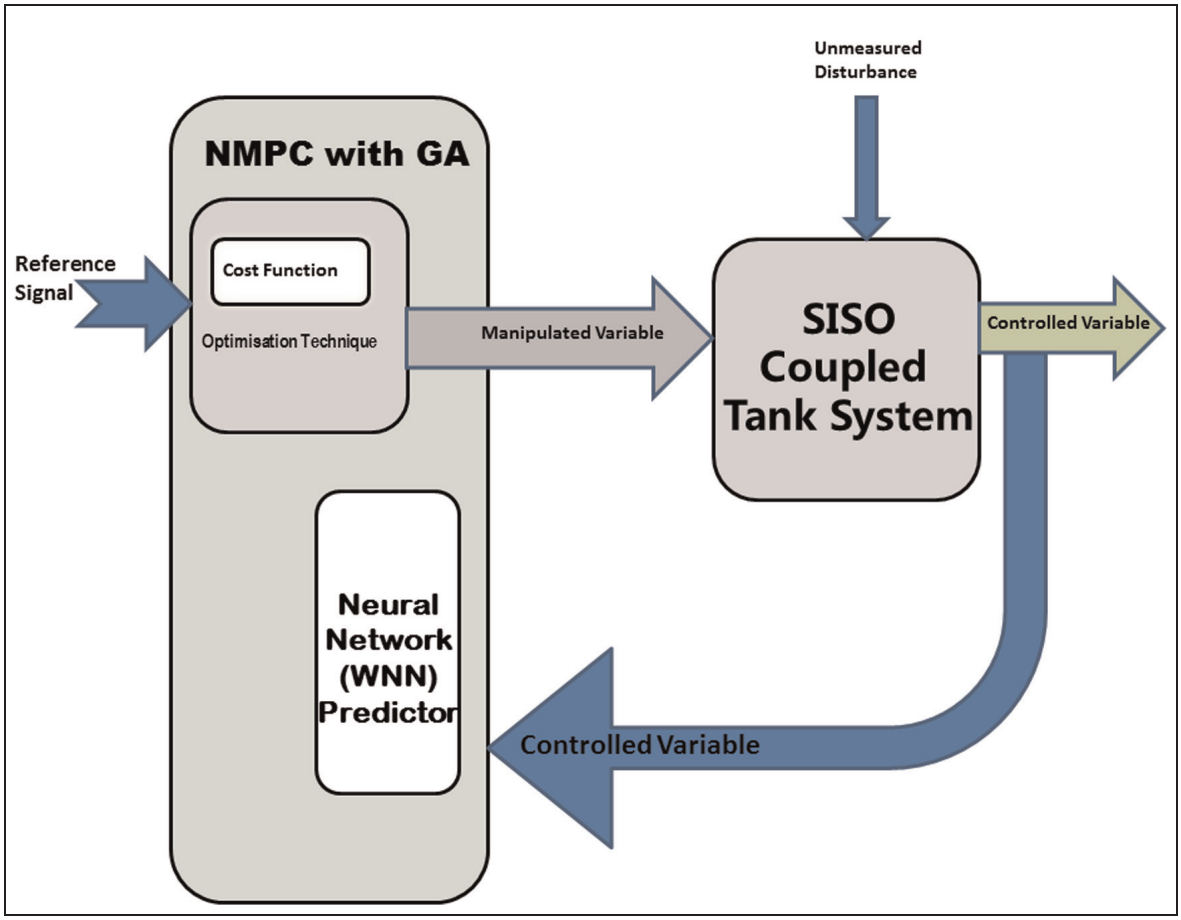

Figure 3. Structure of NMPC with GA optimisation.
SISO: single-input single-output; NMPC: non-linear model predictive control; GA: genetic algorithm.
RTO: Real Time Optimisation.

$$J(\theta) = \left\{ \sum_{i=1}^{p} \left(\sum_{j=1}^{n_y} |w_{i+1,j}^{y}(y_j(k+i+1|k)) - r_j(k+i+1)|^2 + \sum_{j=1}^{n_u} |w_{i,j}^{\Delta u} \Delta u_j(k+i|k)|^2 \right) \right\} \quad (8)$$

The first term in equation (8) represents the error in prediction value and the reference valve, while the second term denotes the change in the previous and the present control efforts. $w_{i+1,j}^{y}$ and $w_{i,j}^{\Delta u}$ are the weights assigned to the set-point tracking and penalty to the change in the inputs, respectively. The GA is used for the RTO process that is done at every sampling instant.

GA implementation

The GA is a stochastic global search method that operates on a population of potential solutions applying the principle of survival of the fittest to evolve a better candidate to a solution. Here, the GA is used to obtain a sequence of optimal manipulated variable control signals that operate the plant. The flowchart for the process involved in GA is shown in Figure 4.

In this work, real-valued genes are used to represent population chromosomes as they provide faster optimisation and use less memory, and there is no need to convert chromosomes to phenotypes before each function evaluation.

Initial populations are generated randomly between the range of 0 and 10 V. This population is created so that the difference between consecutive control horizons is not more than a prescribed value of 1.5 V. These are constraints limiting the range of control signal, whereas the difference between each control inputs into the plant limits the gradient of the control signal. In the case of a minimisation problem, the best individuals will have the lowest numerical value of the associated objective function. Individuals are assigned a fitness value according to their rank in the population in each generation before selections are made. The fitness value is calculated using equation (9)

$$\text{Fitness} = \frac{1}{J+1} \quad (9)$$

Mutation brings variations, diversities and changes in the genetic structures of the overall population, while crossover process interchanges the genetic structure of two or more chromosomes.

In order to deal with real-time implementation constraints, termination measures were implemented to abort the optimisation once a defined sampling time is passed. This invariably might lead to convergence to some sub-optimal/optimal solution within the sampling time period of 0.2 s. The NMPC algorithm is written in such a way that during the RTO process, the best pairs of control horizon vector (population) are constantly retained so that the best population is not destroyed.

The best population is constantly preserved from one generation to the next. After a heuristic search, the optimal parameters for GA that produce results within the sampling interval were selected as follows: population size of 20, generation number of 10, crossover probability of 0.5 and mutation probability of 0.05.[34] In addition, a prediction horizon of 5 and control horizon of 2 are used in the NMPC strategy.

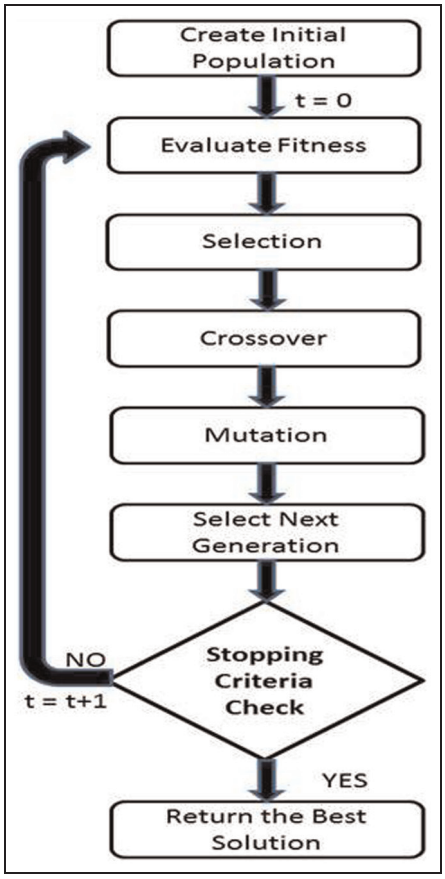

Figure 4. Flowchart of a genetic algorithm procedure.

Results and discussion

The results of the design of an ANN model in previous work[13] with the proposed WNN model are given in Table 2. The results show that both ANN and WNN approaches provided good models for the CTS plant in terms of mean squared error (MSE).

Further results in Figures 5 and 6 are shown to analyse both the approaches in terms of autocorrelation and cross-correlation. Figures 5(a) and 6(a) show the plant output and the model output showing good fitting in both cases, whereas Figures 5(b) and 6(b) show corresponding prediction error between the plant output and the model output. Figures 5(c) and 6(c) are the plots of the autocorrelation of the prediction error. This is used to validate the network performance and gives the indication of how the prediction errors relate in time. For a perfect prediction model in autocorrelation, there should only be one non-zero value of the

Table 2. Training results for both ANN and WNN models.

Performance function (outputs), MSE (m^2)	First data (training)	Second data (validation)	Third data (testing)
ANN[13]	$6.4899e^{-9}$	$6.9932e^{-9}$	$7.1008e^{-9}$
WNN (proposed)	$5.4638e^{-9}$	$1.2002e^{-8}$	$2.0609e^{-8}$

ANN: artificial neural network; WNN: wavelet neural network; MSE: mean squared error.

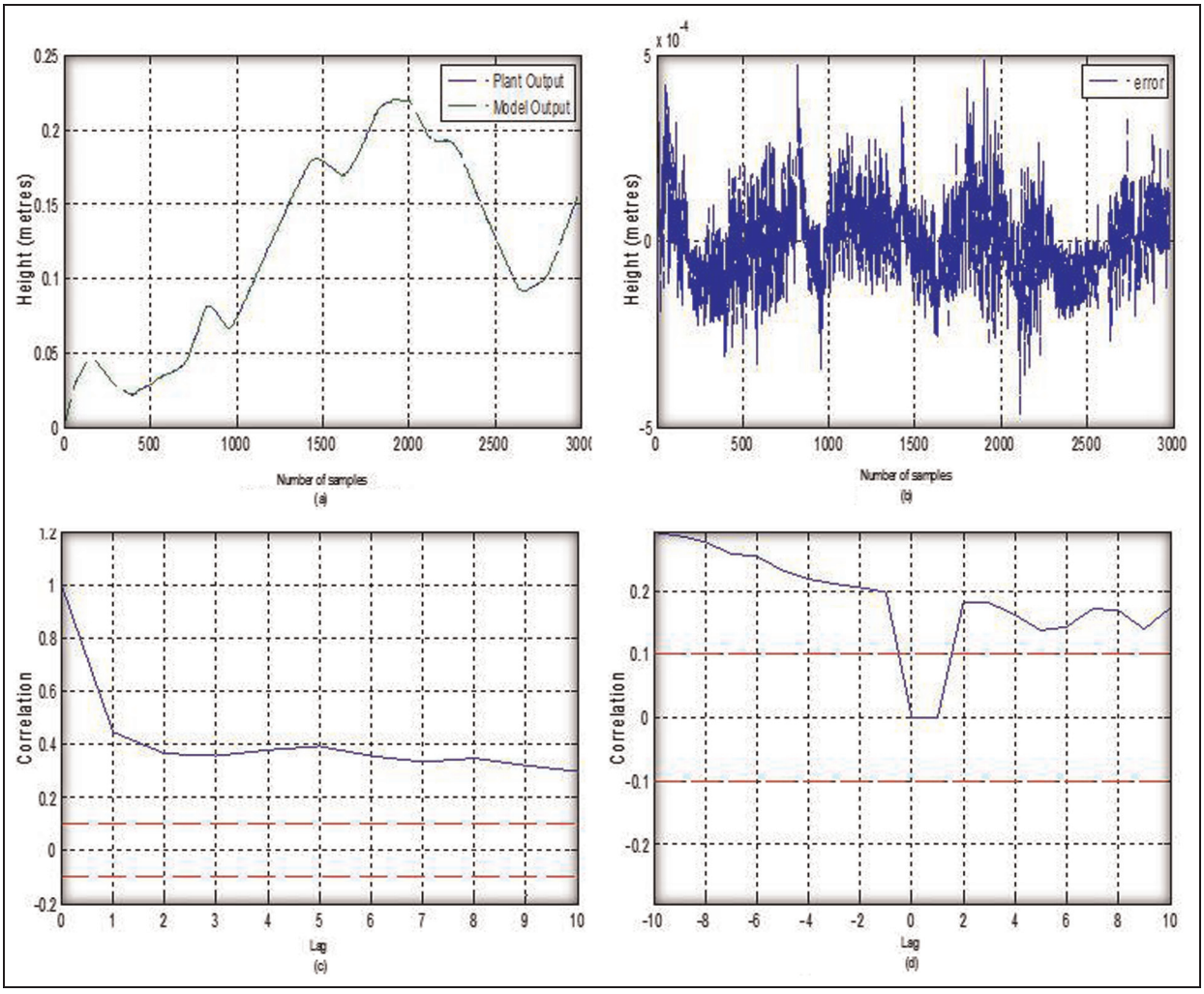

Figure 5. Training results for ANN: (a) plant output and model output, (b) prediction error, (c) autocorrelation of prediction error and (d) cross-correlation of u_1 and prediction error.

autocorrelation function and it should occur at zero lag. This would mean that the prediction errors were completely uncorrelated with each other. In this work, WNN model is closer to the 5% confidence interval (CI) and has 30% more non-zero value of the autocorrelation function at zero lag as compared to ANN model. Figures 5(d) and 6(d) are the plots of the cross-correlation of the prediction error and the training input signal, describing how the prediction errors are correlated with the input sequence u_1. While 100% of WNN model falls within the 10% CI, it is only 10% of the ANN model that falls within the 10% CI. The above results indicate that WNN model is more suitable to tackle non-linear behaviour of the plant compared to ANN model.

Two performance indexes are considered here to evaluate the performance of the NMPC strategy: the Mean Square Error (MSE) and the average control energy (ACE). The MSE is the addition of all the squares of the error differences between the reference and the plant output divided by the total number of samples. This is expressed in equation (10) as

$$\mathrm{MSE} = \frac{\sum_{j=1}^{N} \left(h_{2j}^{r} - h_{2j}^{p}\right)^2}{N} \tag{10}$$

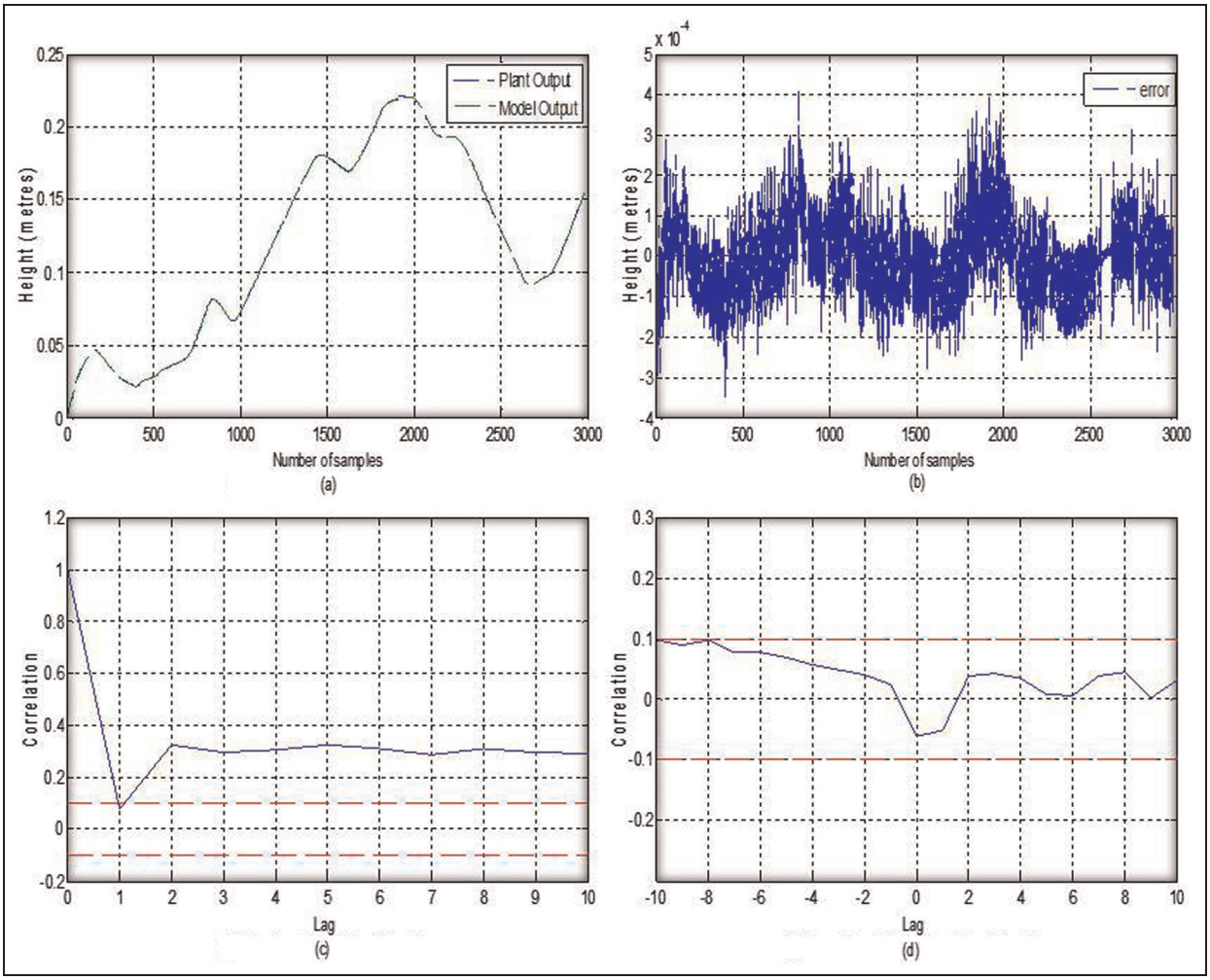

Figure 6. Training results for WNN: (a) plant output and model output, (b) prediction error, (c) autocorrelation of prediction error and (d) cross-correlation of u_1 and prediction error.

In equation (10), superscripts r and p stand for reference value and plant output, respectively, while N stands for the total number of samples. The ACE is defined as the addition of the squares of all the manipulated variables input to the plant divided by the total number of samples and denoted as

$$\mathrm{ACE} = \frac{\sum_{j=1}^{N} u_{1j}^2}{N} \tag{11}$$

Simulation results

The non-linear dynamic equations of the CTS are determined by relating the flow Q_i into the tank to the flow Q_o leaving through the tank valves. Applying the mass balance of flow equation on the tank, it is possible to write this as shown in equation (12)[12]

$$Q_i - Q_o = A\frac{dh}{dt} \tag{12}$$

where A is the cross-sectional area of the tank and h is the height of the fluid in the tank. The unit of equation (1) is expressed in $\mathrm{m}^3\,\mathrm{s}^{-1}$. The flow through the valve can also be expressed as shown in equation (13)[3]

$$Q_o = \delta_x \beta_x \alpha_x \sqrt{2gh_x} \tag{13}$$

where α_x is the cross-sectional area of the orifice; δ_x is the discharge coefficient of the valve; δ_x takes into account all fluid characteristics, losses and irregularities in the systems such that the two sides of the equation balance and β_x is the valve opening expressed as ratio.

At any given time, the heights of fluids in Tanks 1 and 2 relate to the fluid inlet rates and fluid outlet rates. Therefore, equations (12) and (13) can be combined together and applied to Tanks 1 and 2 in order to derive equations (14) and (15), respectively

$$A_1\frac{dh_1}{dt} = K_1 u_1 - \beta_{12}\alpha_{12}\sqrt{(2g(h_1 - h_2))} \tag{14}$$

$$A_2\frac{dh_2}{dt} = -\beta_2\alpha_2\sqrt{2gh_2} + \beta_{12}\alpha_{12}\sqrt{(2g(h_1 - h_2))} \tag{15}$$

Table 3. Physical parameter of the 2nd order SISO coupled tank system.

System parameter of the coupled tank apparatus		
Symbol	Quantity	Value
Tank 1 and Tank 2	Tank cross-sectional area: A_1 and A_2	9.350×10^{-6} m^2
Valves A (α_{12}) and C (α_2)	Valve orifice cross-sectional area	78.50×10^{-6} m^2
β_{12}	Discharge coefficient of 10-mm valve orifice between Tank 1 and Tank 2	1.0
β_2 (Case 1 – normal)	Discharge coefficient of valve C orifice	0.3
β_2 (Case 2 – abnormal)	Discharge coefficient of valve C orifice	1.0
g	Gravitational constant	9.80 m s^{-2}
Liquid level sensors	0 to 10 V DC output corresponds to 0–250 mm height	
Pump flow sensors	0 to 10 V DC output corresponds to 0–4400 cm^3 min^{-1}	

DC: direct current.

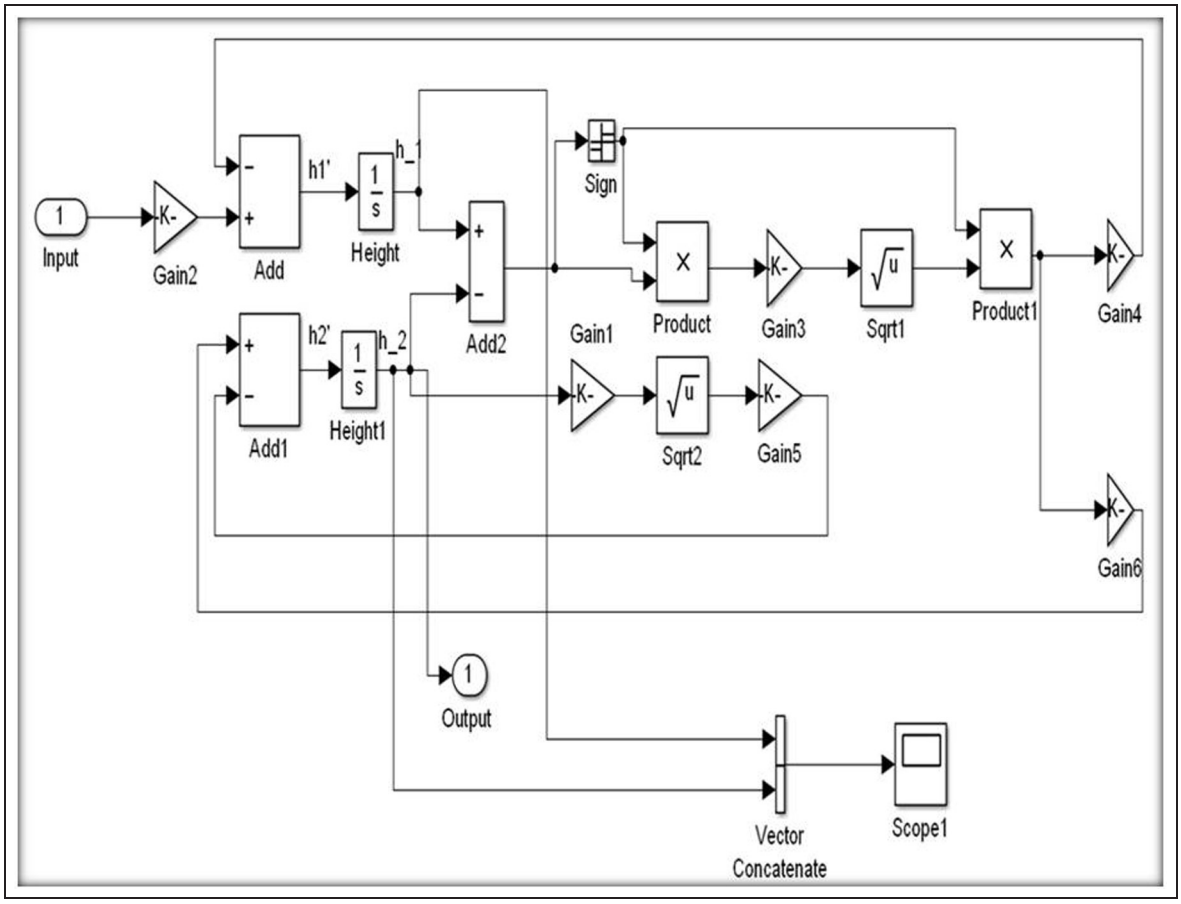

Figure 7. SISO coupled tank system in Simulink® design.

where A_1 and A_2 are the cross-sectional areas, h_1 and h_2 are the water levels of Tanks 1 and 2, respectively, and K_1 is the pump constant expressed in $m^3\,V^{-1}\,s^{-1}$ unit. The discharge coefficients (β) of the valve take into account the fluid characteristics, losses and irregularities in the system such that the two sides of the equation balance and cancel out.

The physical parameters of the TQ CE105MV CTS are provided in Table 3. In order to implement the simulation of the NMPC strategy successfully, the SISO CTS non-linear equations (14) and (15) are used in combination with the CTS physical parameters to design the Simulink® diagram as shown in Figure 7.

The single input is u_1 and single output is h_2. This representation of the plant will be used in simulation of the NMPC strategy.

The ANN and WNN models were first tested in NMPC strategies to track the whole operating regions with reference points ranging from 1 to 20 cm of height of water in the second tank. The MSE obtained is $1.838 \times 10^{-4}\,m^2$ for the ANN-NMPC strategy and $1.1806 \times 10^{-4}\,m^2$ for the WNN-NMPC strategy, whereas the ACE is $27.131\,V^2$ for the ANN-NMPC and $26.732\,V^2$ for the WNN-NMPC strategy. The results indicate that WNN-NMPC is able to track different reference points in the operating regions and is

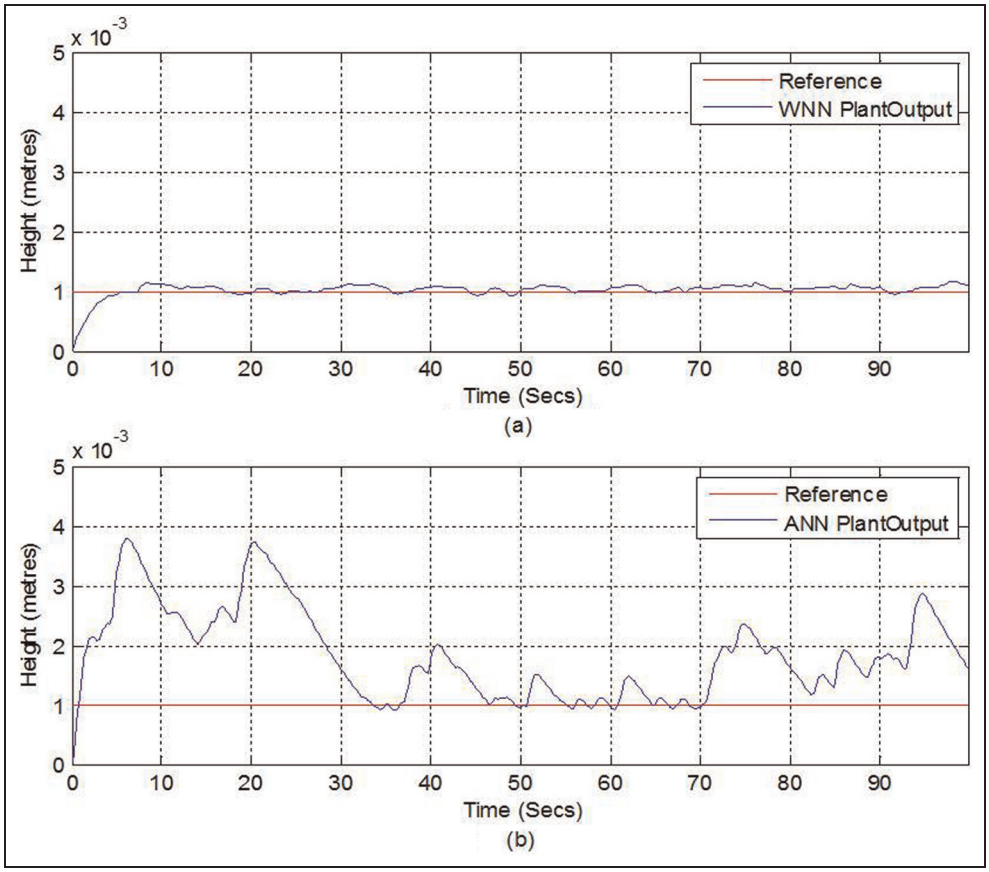

Figure 8. Case 1: ANN/WNN NMPC simulation tracking of 1 mm level: (a) WNN model and (b) ANN model.
WNN: wavelet neural network; ANN: artificial neural network.

more effective both in terms of MSE and ACE compared to ANN-NMPC.

Two case scenarios are studied in this article.

Case 1. This is the normal case where valve C is opened midway position ($\beta_2 = 0.3$). The NMPC strategy was applied to control the high height (1 mm) of the fluid in Tank 2 with both tanks at initial zero levels.

Case 2. This is the abnormal situation of worst-case scenario. Both tanks were initially pumped with fluid to 5 cm level. From the start of the experiment, two valves B and C are all left fully closed, while valve A is fully opened. The NMPC strategy was then applied to control the same high height. Precisely, after 1 s (5 sampling instants) of operations, valve C is then fully opened ($\beta_2 = 1.0$) to create abnormal situation such as valve failure. This situation creates a different dynamics from the initial data trained.

The performance of both strategies will now be tested in maintaining the height of very low level of water in the second tank.

Figure 8(a) and (b) shows the comparison of the simulation response results of using both WNN and ANN models, respectively, for the NMPC strategies (Case 1) tracking an extremely low height (0.4% of the tank's height) such as 1.0×10^{-3} m or 1 mm.

The MSE obtained is $1.26 \times 10^{-6}\,\mathrm{m}^2$ for the ANN-NMPC strategy, while it is $1.44 \times 10^{-8}\,\mathrm{m}^2$ for the WNN-NMPC strategy for low-level control. The result shows that the WNN-NMPC strategy is more effective and with no overshoot in maintaining the extremely small level in comparison to the ANN-NMPC strategy. Moreover, the ACE is $1.65\,\mathrm{V}^2$ for the ANN-NMPC strategy, while it is $0.13\,\mathrm{V}^2$ for the WNN-NMPC strategy. The WNN-NMPC strategy thus uses 90% less controller energy in comparison to the ANN-NMPC strategy.

Similarly, Figure 9(a) and (b) shows the comparison of the simulation response results for Case 2. The comparison results are similar, and this is expected because of the initial starting levels. Also, the level tracking is more precise because of the level has settled before the tracking starts. WNN still performs better even though they have close MSEs and ACEs values (see Table 4).

Real-time implementation

In order to carry out the real-time practical implementation of the simulations in the earlier sections, an experimental set-up of CE105MV multi-variable CTS

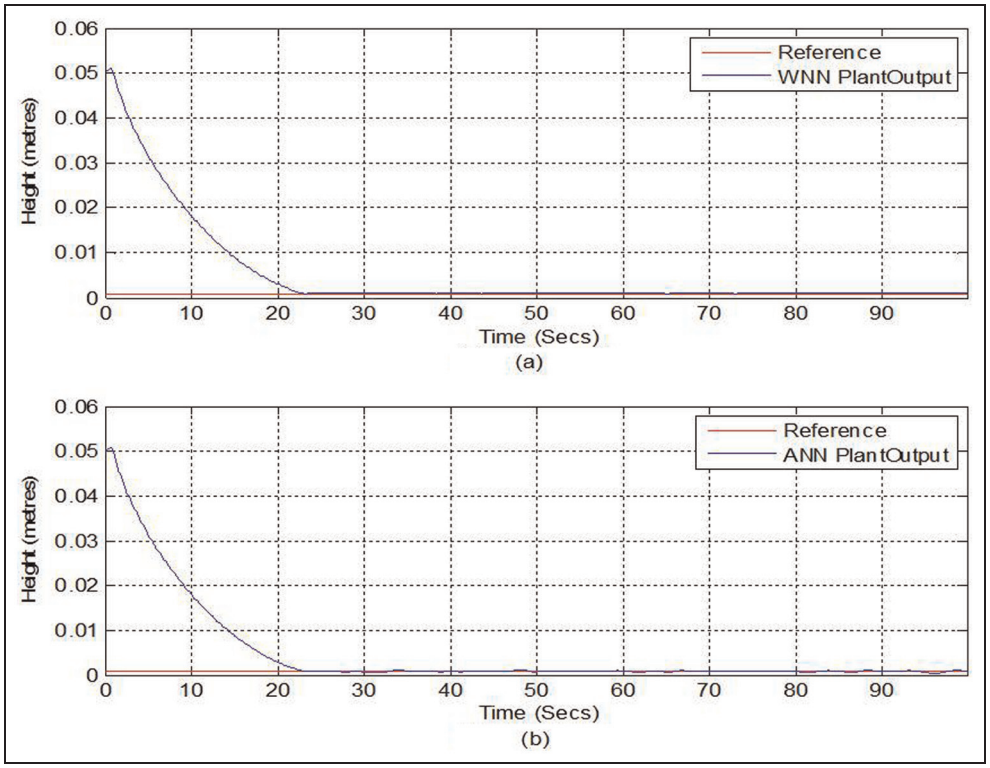

Figure 9. Case 2: ANN/WNN NMPC simulation tracking of 1 mm level: (a) WNN model and (b) ANN model.
WNN: wavelet neural network; ANN: artificial neural network.

Table 4. Simulation and real-time results for ANN/WNN NMPC strategies.

	Case 1 (normal)				Case 2 (abnormal)			
	Simulation		Real-time		Simulation		Real-time	
	MSE (m^2)	ACE (V^2)	MSE (m^2)	ACE (V^2)	MSE (m^2)	ACE (V^2)	MSE (m^2)	ACE (V^2)
ANN	$1.26e^{-6}$	1.65	$7.30e^{-6}$	7.62	$1.25e^{-4}$	2.16	$2.09e^{-4}$	16.24
WNN	$1.44e^{-8}$	0.13	$1.04e^{-6}$	3.27	$1.23e^{-4}$	1.35	$1.51e^{-4}$	15.59

ANN: artificial neural network; WNN: wavelet neural network; MSE: mean squared error; ACE: average control energy.

from TecQuipment (TQ) is used. This equipment is shown in Figure 10(a), while its schematic diagram is shown in Figure 10(b). A data acquisition (DAQ) card (NI 6009) from National Instruments with a LabVIEW® software driver is configured to acquire real-time SISO sensor data and to send the manipulated input to control the fluid level in Tank 2. The pump input voltage ranges between 0 and 12 V, whereas in this work, a maximum of 10 V is used for safety purposes. A computer laptop with an Intel® Core™ i5-2410M central processing unit (CPU) of 2.30 GHz and 6.0 GB of random-access memory was used for testing in real time. The CE105MV unit comprises two variable speed pumps and two tanks connected by a variable area channel and drain valves to a sump located in the base of the equipment. There are two calibrated piezo-resistive silicon pressure–type depth transducers (level sensors), an electronic flow metre and a variable area gap flow metre to provide visual indication of flow rate. The control strategy is designed in a way that the rate of change of the control input is controlled in small steps to avoid major fluctuations. This can be achieved by the manipulation of pump inputs and by varying the sectional area of rotary valves A and C, as shown in Figure 10(a) and (b).

Real-time results. Section 'Results and discussion' shows that the WNN-NMPC strategy performs well in terms of both MSE and ACE compared to the widely used ANN-NMPC strategy and is able to maintain low level without much fluctuations. A real-time experiment is performed in this section to verify the result. Figure 11(a) and (b) shows the comparison of the real-time response results of both the WNN and ANN models, respectively, for the NMPC strategies (Case 1). The MSE is $7.30 \times 10^{-6}\,m^2$ for the ANN-NMPC strategy, while it is $1.04 \times 10^{-6}\,m^2$ for the WNN-NMPC

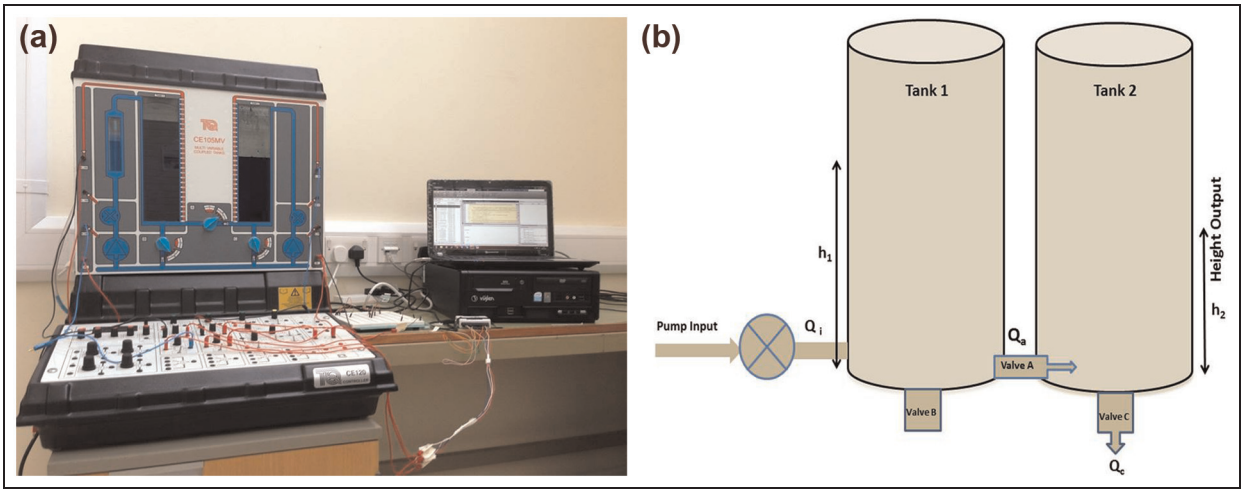

Figure 10. Coupled tank system (CTS): (a) experimental set-up of the CTS and (b) schematic diagram of the SISO CTS.

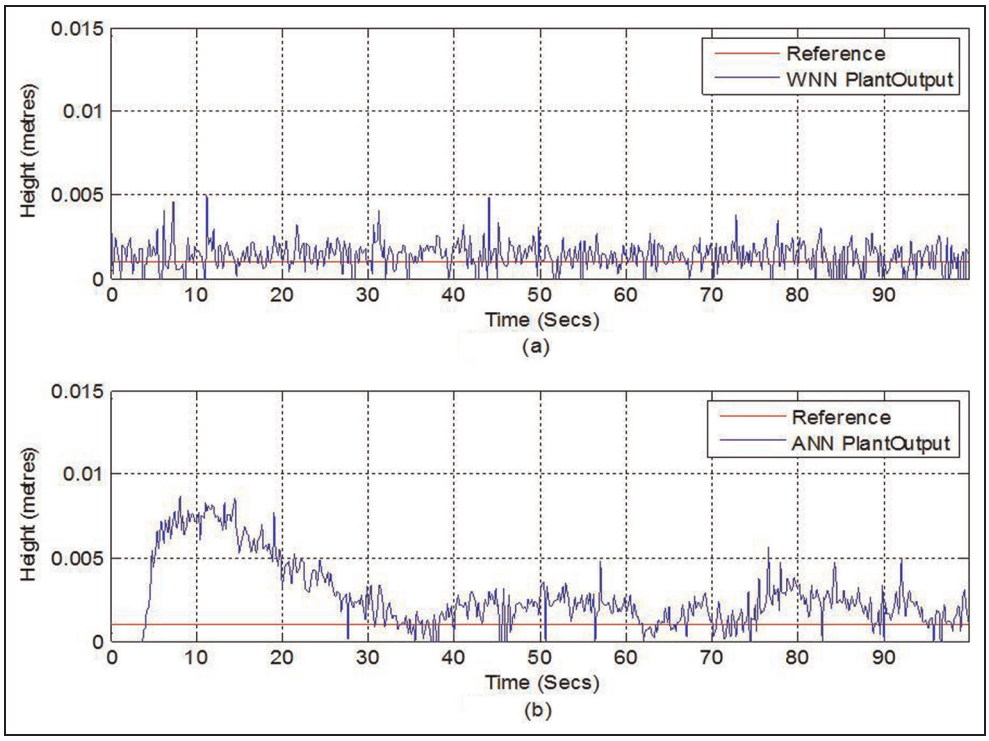

Figure 11. Case 1: ANN/WNN NMPC real-time tracking of 1 mm level: (a) WNN model and (b) ANN model.
WNN: wavelet neural network; ANN: artificial neural network.

strategy. This confirms that WNN-NMPC strategy has more efficient tracking capabilities of extremely small heights over the ANN-NMPC strategy both in simulation and in real time.

Moreover, the ACE is 7.62 V^2 for the ANN-NMPC strategy, while it is 3.27 V^2 for the WNN-NMPC strategy, showing it is 50% more energy efficient compared to ANN-NMPC. WNN-NMPC thus needs one-half the amount of controller energy expended in real time by ANN-NMPC in order to maintain the low-level height of 1 mm as set point.

Similarly, the practical implementation is carried out for Case 2 scenario. Figure 12(a) and (b) compares the response of the NMPC strategies for both WNN and ANN models. Also, similar explanation to the simulation case applies here. WNN has lower MSEs and ACEs also in this case (see Table 4).

Concluding remarks

This work has demonstrated, both in simulation and in real-time implementation, a novel model based on WNN-NMPC strategy for maintaining the height of the liquid at very low level. In order to further handle the difficulties in network training and achieving a global optimal solution, a fast effective stochastic wavelet

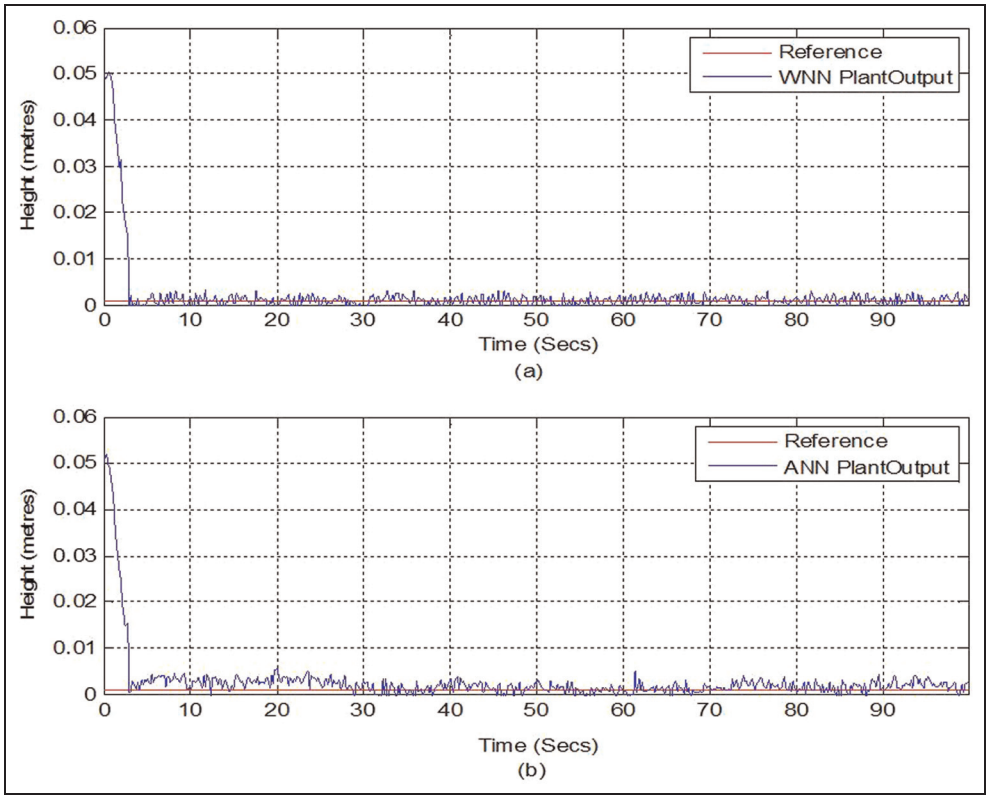

Figure 12. Case 2: ANN/WNN NMPC real-time tracking of 1 mm level: (a) WNN model and (b) ANN model.
WNN: wavelet neural network; ANN: artificial neural network.

gradient algorithm is employed for initial network training. The GA is further used for the final optimisation of wavelet networks weights, which include the dilation and translation parameters. This approach can sufficiently prevent the training process from becoming trapped in a local minimum solution because a global search method was used for the initial starting weights for the wavelet gradient algorithm. The obtained reliable non-linear model of the CTS showed the effectiveness of the WNN over an ANN model especially in the control strategy of extremely small fluid volume where non-linearities are high. In addition, WNN-NMPC is effective in set-point tracking and actuation efficiency. The whole strategy is well suited for chemical processes with varying interaction rates. The SISO system can easily be upgraded to multi-input multi-output (MIMO) system, while the same underlying principle can easily be applied to model other industrial processes. Both strategies performed well in abnormal scenarios, and this gives an indication of the usefulness in case of valve malfunctions or total valve failure. The proposed controller is efficient under the worst-case valve position and will work under different valve settings.

Most importantly, the novel WNN-NMPC strategy has the potential to have improved performance for more complex non-linear MIMO problems than the ANN-NMPC strategy.

Declaration of conflicting interests

The authors declare that there is no conflict of interest.

Funding

Petroleum Training Development Fund (PTDF), Nigeria, funded this study.

References

1. Mohideen KA, Saravanakumar G, Valarmathi K, et al. Real-coded genetic algorithm for system identification and tuning of a modified model reference adaptive controller for a hybrid tank system. *Appl Math Model* 2013; 37(6): 3829–3847.
2. Braatz RD. Control of fluids. *IEEE Contr Syst Mag* 2013; 33(1): 8–9.
3. Laubwald E. Coupled tank system. *Control Syst Princ* 2005; 1: 1–8.
4. Nawi SM, Abdalla AN and Ramli MS. Improved coupled tank liquid levels system based on hybrid genetic-immune adaptive tuning of PI controller. In: *International conference on electrical, control and computer engineering (INECCE)*, Pahang, Malaysia, 21–22 June 2011, pp.247–252. New York: IEEE.
5. Khalid MU and Kadri MB. Liquid level control of non-linear coupled tanks system using linear model predictive control. In: *2012 International conference on emerging technologies*, Islamabad, Pakistan, 8–9 October 2012, no. 1, pp.1–5. New York: IEEE.

6. Holič I and Veselý V. Robust PID Controller Design for Coupled-Tank Process. In: Fikar M and Kvasnica M (eds) *Proceedings of the 18th International Conference on Process Control*, Hotel Titris,Tatranská Lomnica, Slovakia, 14–17 June 2011, pp. 506–512.
7. Meyrick CW and Rekate HL. Cerebrospinal fluid control system. *P IEEE* 1988; 76(9): 1226–1235.
8. Pluta J and Sibielak M. The application of a piezoelectric stack for control of small flow intensity hydraulic fluid. In: *Proceedings of the 13th international Carpathian control conference*, High Tatras, 28–31 May 2012, pp.573–577. New York: IEEE.
9. Long J, Ji H, Wang B, et al. Online parameters measurement of Taylor flow in small channels using optical technique. In: *2012 IEEE international instrumentation and measurement technology conference*, Graz, 13–16 May 2012, pp.2322–2325. New York: IEEE.
10. TecQuipment. CE105MV, Control engineering, sensors and instrumentation, 2013, pp.1–3.
11. Heckenthaler T and Engell S. Approximately time-optimal fuzzy control of a two-tank system. *IEEE Control Syst Mag* 1994; 14(3): 24–30.
12. Anthony AR, Paulo RM, Jorge DD, et al. Reinforcement learning for controlling a coupled tank system based on the scheduling of different controllers. In: *Proceedings of the 2010 eleventh Brazilian symposium on neural networks*, São Paulo, Brazil, 23–28 October 2010, pp.212–216. New York: IEEE.
13. Owa K, Sharma SK and Sutton R. Non-linear model predictive control strategy based on soft computing approaches and real time implementation on a coupled-tank system. *Int J Adv Res Comput Sci Softw Eng* 2013; 3(5): 1350–1359.
14. Al-Qaisy MAS. Linear and non-linear multi-input multi-output model predictive control of continuous stirred tank reactor. *Tikrit J Eng Sci* 2012; 19(3): 41–57.
15. Rahmat MF and Rozali SM. Modeling and controller design for a coupled-tank liquid level system: analysis and comparison. *Jurnal Teknologi*, 2008; 48(D): 113–141.
16. Gupta H and Verma OP. Intelligent controller for coupled tank system. *Int J Adv Res Comput Sci Softw Eng* 2012; 2(4): 154–157.
17. Tran TH, Nguyen MT, Kwok NM, et al. Sliding mode-PID approach for robust low-level control of a UGV. In: *International conference on automation science and engineering*, Shanghai, China, 8–10 October 2006, pp.672–677. New York: IEEE.
18. Findeisen R and Allgower F. An introduction to nonlinear model predictive control. *Control* 2002; 11: 1–23.
19. Tricaud C. Linear and nonlinear model predictive control using a general purpose optimal control problem solver RIOTS 95. In: *2008 Chinese control and decision conference*, Yantai, China, 2–4 July 2008, pp.1552–1557. New York: IEEE.
20. Richalet J. Industrial applications of model based predictive control. *Autom* 1993; 29(5): 1251–1274.
21. Kosanovich KA, Piovoso MJ, Rokhlenko V, et al. Nonlinear adaptive control with parameter estimation of a CSTR. *J Process Contr* 1995; 5(3): 137–148.
22. Alvarado I, Limon D, Ferramosca A, et al. Robust tubed-based MPC for tracking applied to the quadruple-tank process. In: *17th IEEE international conference on control applications part of IEEE multi-conference system control*, San Antonio, TX, 3–5 September 2008, vol. 3, no. 3, pp.305–310. New York: IEEE.
23. Kubalcik M and Bobal V. Adaptive control of three tank system: comparison of two methods. In: *16th Mediterranean conference on control and automation*, Ajaccio, 25–27 June 2008, pp.1041–1046. New York: IEEE.
24. Monteiro JRBA, Suetake M, Paula GT, et al. Wind velocity neural estimator for small autonomous surface vehicles. In: *Second Brazilian conference on critical embedded systems*, Campinas, Brazil, 20–25 May 2012, pp.6–11. New York: IEEE.
25. Alzahra Z and Dashti S. Neural adaptive control for electro hydraulic servo system. In: IEEE international conference, *Control Conference (ASCC), 9th Asian*, Istanbul 23–26 June 2013, pp.16
26. Shrivastava P and Trivedi A. Control of nonlinear process using neural network based model predictive control. *Int J Eng Sci Technol* 2011; 3(4): 2573–2581.
27. Cheng-Jian L, Cheng-Chung C and Cheng-Ling L. A wavelet-based neuro-fuzzy system and its applications. In: *Proceedings of the IEEE international joint conference on neural networks*, Volume 3, 20–24 July 2003, pp.1921–1926. New York: IEEE.
28. Coca D and Billings SA. System identification using wavelets. *Control Syst Robot Autom* 2012; 6: 1–10.
29. Lu J, Gu Z and Wang H. Research on the application of the wavelet neural network model in peak load forecasting considering the climate factors. *Proceedings of the Fourth International Conference on Machine Learning and Cybernetics*, Guangzhou, 18–21 August 2005, pp.538–543. New York: IEEE.
30. Lilong W, Dongfang X, Hao S, et al. Application of optimized wavelet neural network based on genetic algorithm in stock market prediction, no. 1, 1990, pp.1–4.
31. Jahangiri F, Doustmohammadi A and Menhaj MB. Identification of twin-tanks dynamics using adaptive wavelet differential neural networks. *Neurocomputing* 2012; 77: 12–19.
32. Meng M and Sun W. Short-term load forecasting based on rough set and wavelet neural network. In: *2008 international conference computational intelligence and security*, Suzhou, China, 13–17 December 2008, pp.446–450. New York: IEEE.
33. Tani T, Murakoshi S and Motohide U. Neuro-fuzzy hybrid control system of tank level in petroleum plant. *IEEE T Fuzzy Syst* 1996; 4(3): 360–368.
34. Pham D and Karaboga D. *Intelligent optimisation techniques*. London: Springer Books, 2000.